2019 SECED Conference
Earthquake risk and engineering towards a resilient world
9-10 September 2019, Greenwich, London

VULNERABILITY ASSESSMENT OF RC STRUCTURES INCLUDING NONLINEAR SOIL-STRUCTURE INTERACTION EFFECTS

Christos PETRIDIS[1] & Dimitris PITILAKIS[2]

Abstract: *To date, significant research projects aim towards a resilient, low-risk built environment, leading to a significant number of seismic fragility and vulnerability assessment studies. However, in most cases, the influence of the underlying soil conditions remains vague. Our purpose is to evaluate the effects of fully nonlinear soil-structure interaction (SSI) on urban-scale earthquake vulnerability of reinforced concrete (RC) buildings, i.e. accounting for the nonlinear behavior of the foundation-soil and the structure, as well as soil-structure interaction. While these effects might be included in building-specific analyses, large-scale risk assessment typically neglects them. To this end, we exploit a set of fragility modifiers that appropriately transpose existing fragility curves for RC buildings to consider the influence of nonlinear SSI. The use of fragility modifiers enables the engineer to easily consider soil-related effects, without the need to run individual building-to-building analyses. The results are presented in the form of loss/vulnerability curves, indicating the differences that occur because of nonlinear SSI. A key finding of this work is the differences that occur when SSI and nonlinear soil behavior are taken into account, as well as the efficiency of the fragility modifiers for risk assessment.*

Introduction

Seismic risk assessment has evolved into an indispensable tool for engineers, insurance companies, government, and civil protection organisations under the umbrella of disaster risk reduction (DRR), ranging from building-specific to global-level maps (GEM 2019). Relatively rare earthquake events of great magnitude imply lack of data regarding earthquake losses and damage, especially when it comes to individual structural typologies, subsoil conditions and other particularities that further filter the available data. On the other hand, numerical models represent a nearly-always feasible way to assess seismic risk. In specific, various fragility and vulnerability functions have already been developed (Yepes-Estrada et al. 2016), covering a wide variety of structural typologies met worldwide. However, subsoil-specific studies of this extend are not available and soil-structure interaction (SSI) effects are rarely included (Rajeev and Tesfamariam 2012, Karapetrou et al. 2015, Petridis and Pitilakis 2018 and Pitilakis and Petridis 2018), consequently, generic fragility functions are usually adopted, only parameterized in terms of the building typologies. To bridge the gap between different structural typologies and typical subsoil profiles, we select eighteen reinforced concrete building typologies and seven soil profiles – all of them representing common engineering practice – to derive the fragility and vulnerability curves of every combination possible. Furthermore, to avoid complexing the problem, instead of providing 126 building- and soil-specific sets of fragility curves, we focus on quantifying the differences that occur between the fixed-base models and the ones studied. To ensure a direct and convenient scheme for the application of our results – e.g. using OpenQuake (Silva et al. 2014) – we provide a set of fragility modifiers that appropriately change soil-independent fragility curves found in the literature by multiplying their median values, accounting for nonlinear soil behavior and SSI effects. In this paper, we present the results obtained from this extensive work, post-processed in terms of vulnerability.

[1] PhD Candidate, Aristotle University of Thessaloniki, Thessaloniki, Greece, cpetridi@civil.auth.gr
[2] Assistant Professor, Aristotle University of Thessaloniki, Thessaloniki, Greece

Methodology

Buildings covered

In this study, we adopt Kappos et al. (2006) reinforced concrete building typologies to cover the corresponding structural typologies met in common engineering practice. In particular,

- Regarding the lateral load resisting system, both moment resisting frames and dual (frame + shear wall) structures are examined.
- Regarding the height of the buildings, low-rise, mid-rise and high-rise models are investigated.
- Regarding the infills, bare, regularly infilled and soft-storey (pilotis) configurations are adopted.
- Regarding the seismic code, all the models are assumed to be designed and constructed under the provisions of the "Royal Decree of 1959, Greece", namely a low-code, nonductile design is expected.

In this manner, we model using OpenSEES (Mazzoni et al. 2009) a set of 18 buildings, including the material nonlinearities involved via the use of the fiber elements provided. Common, square-shaped footings are selected as the indicative foundation type of the low-code buildings examined.

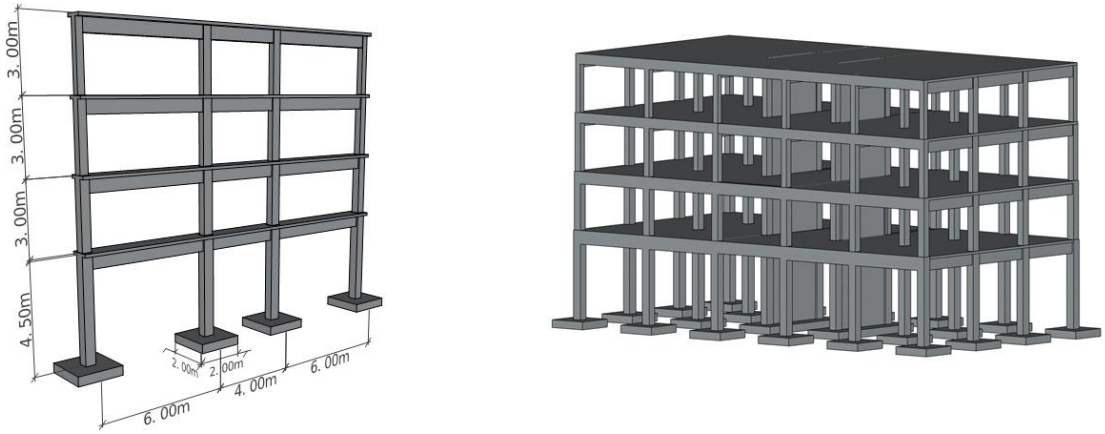

Figure 1. Sketch of the structural typologies examined, with respect to the lateral load resisting mechanism; left: moment resisting frame, right: dual (frame + shear wall) system.

Soil profiles covered

All the investigated building models are combined with different subsoil profiles to study the effects of both nonlinear soil behavior and SSI on the fragility and vulnerability curves subsequently derived. We select a non-symmetric range of soil models, parameterized in terms of the shear wave velocity, extending from rock to very soft clays. Based on the assumption that SSI is mostly apparent on soft soil conditions, the set of soil profiles selected is soft-soil-skewed. Using OpenSEES, each soil profile is modelled as a pseudo-1D equivalent of the physical free-field to transfer the ground motion from the underlying bedrock to the surface. "PressureIndependMultiYield" material is adopted to account for nonlinear soil behavior.

Accordingly, the characteristics of the soil profiles affect the definition of the beam-on-nonlinear-Winkler foundation springs, used to capture SSI effects at the foundation level; upon definition, these spring elements are assigned at the base of each footing to create the flexible-base models. Since this study focuses on quantifying the effects of soil-foundation flexibility, the corresponding fixed-base models are further developed to act as a reference, assuming that all foundation degrees of freedom are restrained. Table 1 presents the seven soil profiles selected, classified according to EN 1998-1.

Table 1. Shear wave velocity and classification of the soil profiles

No.	**1.**	**2.**	**3.**	**4.**	**5.**	**6.**	**7.**
Vs (m/s)	>800	450	360	300	250	180	150
Type (EC8)	A	B	C	C	C	D	D

Dynamic analyses

Incremental Dynamic Analysis (IDA) is performed to derive a cloud of intensity measure (IM) against engineering demand parameter (EDP) pairs (Vamvatsikos and Cornell 2002, Vamvatsikos and Cornell 2004). We select PGA referring to the underlying bedrock as the IM and maximum interstory drift (maxISD) as the EDP. Qualifying PGA on rock conditions as IM facilitates highlighting the differences introduced by soil nonlinearities; the use of maxISD as the EDP provides an efficient overview of the damage at global level. For the IDA the input ground motions are scaled at bedrock level from 0.0 to 1.0g by a constant step of 0.05g. Table 2 presents the ground motions used, all of them recorded on sites classified as rock.

Table 2. Earthquake recordings.

No.	**Location**	**Database Code**	**R_{epi} (km)**	**M_w**	**PGA (m/s^2)**	**Vs,30 (m/s)**	**Soil (EC8)**
1	Tabas/Iran	ESMD_59	12.00	7.35	3.16	826.00	A
2	Montenegro/Montenegro	ISESD_223	21.00	6.90	1.77	1083.00	A
3	App.Lucano/Italy	ITACA_614	9.80	5.60	1.62	1024.00	A
4	Kobe/Japan	NGA_1108	25.40	6.90	2.85	1043.00	A
5	Sierra Madre/Mexico	NGA_1645	6.46	5.61	2.71	821.69	A
6	Loma Prieta/USA	NGA_3548	20.35	6.93	4.12	1070.34	A
7	Whittier Narrows/USA	NGA_680	13.85	5.99	1.10	969.07	A
8	Northridge/USA	NGA_994	25.42	6.69	2.84	1015.88	A
9	Izmit/Turkey	T-NSMP_1109	3.40	7.60	1.65	826.11	A
10	East Sicily/Italy	ITACA_314	28.30	5.60	0.61	871.00	A
11	Western Tottori/Japan	KIK-Net_3775	31.37	6.60	1.55	967.27	A

Fragility assessment

Fragility curves represent the probability of exceeding a predefined limit state, as a function of an engineering demand parameter, under a seismic excitation of given intensity. Equation 1 describes the cumulative conditional probability of exceeding a DS for a given IM.

$$P[DS|IM]=\Phi\left(\frac{\ln(IM)-\ln(\overline{IM})}{\beta}\right) \quad (1)$$

where Φ is the standard normal cumulative distribution function, IM is the intensity measure of the earthquake expressed in terms of PGA, $\overline{IM}$ is the corresponding median value, β is the log-standard deviation and DS is the damage state. In particular, the log-standard deviation parameter β characterizes the total dispersion related to each fragility curve. There are three primary sources of uncertainty which contribute to the total variability of any given limit state (NIBS 2004); (i) the variability related to the definition of the limit state value, (ii) the capacity of each structural model and (iii) the seismic demand. The log-standard deviation referring to the definition of the limit states is equal to 0.40 and the corresponding value regarding the capacity is assumed equal to 0.30 for structural systems designed with no/low seismic code (NIBS 2004). The latter source of uncertainty, associated with the seismic demand, is explicitly evaluated estimating the dispersion for the logarithms of PGA – maxISD pairs, with respect to the selected regression method.

We adopt four damage states, namely Slight Damage (SD), Moderate Damage (MD), Extensive Damage (ED) and Complete Damage (CD) (D'Ayala et al. 2013).

Fragility modifiers

Fixed-base and flexible-base fragility curves

With a view to quantifying the differences between the (i) flexible- (SSI-inclusive) and (ii) the fixed-base models, fragility curves for each damage state are derived for both models. Flexible-base fragility curves inherently include any site amplification effects observed.

Derivation of fragility modifiers (FM)

While a comprehensive fragility assessment, including subsoil conditions and foundation flexibility, is a feasible task for building-specific purposes, the use of this methodology for large-scale risk assessment, e.g. urban-scale, is a cumbersome procedure. To this end, we derive a set of fragility modifiers (FM) that appropriately shift the existing fragility curves to take into account nonlinear soil behavior and SSI effects. Having derived the fragility curves for all the cases studied, we estimate the ratios between the PGAs associated with 50% probability of exceeding each damage state. This way, we estimate how much the risk analyst has to shift the existing fixed-base fragility curve to approach the flexible-base one, without going into further numerical calculations. The inherent uncertainties are found to be similar between the fixed- and flexible-base models, and thus, we propose a simple transpose of the fragility curves by multiplying the PGA at 50% probability of exceedance with the estimated FM, without affecting the inclination of the curve, i.e. assuming that variability remains the same. In essence, the proposed FM are the result of this extensive procedure which estimates the ratios between all studied cases. Equation 2 describes the calculation behind the derivation of the FM.

$$FM_i = \frac{PGA_{50\%,\text{flexible-base,i}}}{PGA_{50\%,\text{fixed-base,i}}} \quad (2)$$

in which, *i* loops over Slight Damage (SD), Moderate Damage (MD), Extensive Damage (ED) and Complete Damage (CD), $PGA_{50\%,\text{flexible-base}}$ is the peak ground acceleration at the underlying bedrock corresponding to 50% probability of the flexible-base-on-soil model to exceed a given damage state *i*, and $PGA_{50\%,\text{fixed-base}}$ is its fixed-base-on-rock counterpart. Figure 2 presents the FM including both nonlinear soil behavior and SSI effects.

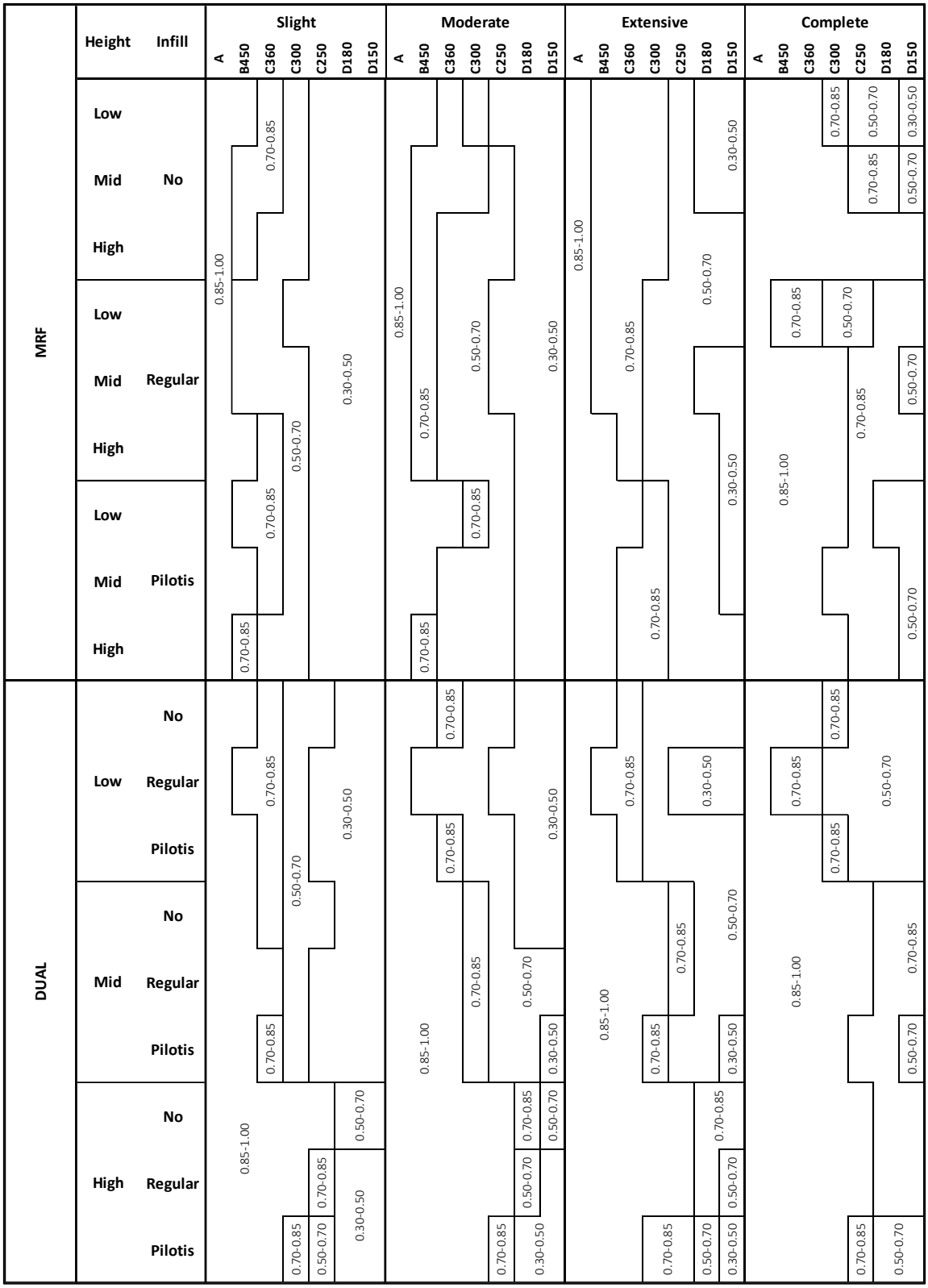

Figure 2. Fragility modifiers from fixed-base-on-rock to flexible-base-on-soil (nonlinear soil behavior and SSI) transition.

Application of fragility modifiers on existing fragility curves

Illustratively, we use as a benchmark the fragility curves derived by Kappos et al. (2006) to apply the FM estimated. Assuming that the damage states selected comply with the ones adopted in this study, in terms of the damage description, one may practically use any fragility curves existing in the literature.

Figure 3 shows the fragility curves derived by Kappos et al. (2006) and the ones derived applying the FM proposed for a four-storey, dual, regularly infilled building resting on type C (V_s=300m/s) soil. Figure 4 shows the fragility curves derived by Kappos et al. (2006) and the ones derived applying the FM proposed for a four-storey, dual, regularly infilled building resting on type D (V_s=180m/s) soil. Using Figure 2, e.g. for the four-storey, dual, regularly infilled building resting on type D (Vs=180m/s) soil and for the MD damage state, we estimate a FM ranging from 0.50 to 0.70 (mean at 0.60). The PGA corresponding to the median value for the respective Kappos et al. (2006) curve is $PGA_{50\%,fixed\text{-}base}$= 3.4 m/s^2 (Figure 4); multiplying the $PGA_{50\%,fixed\text{-}base}$ by FM we estimate $PGA_{50\%,flexible\text{-}base}$= 2.04 m/s^2 (Figure 4).

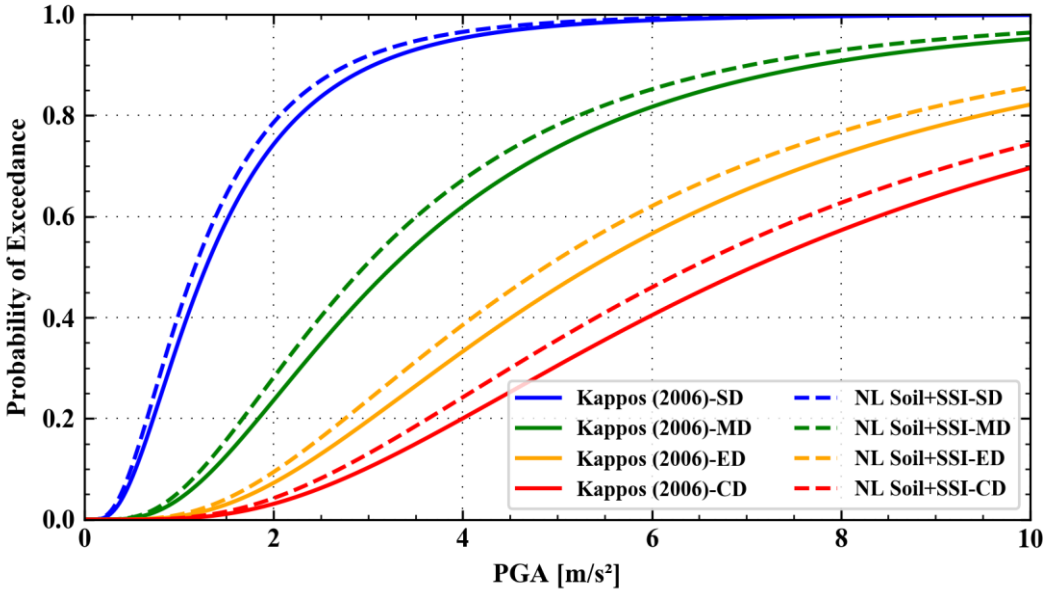

Figure 3. Fragility curves derived by Kappos et al. (2006) and the ones derived applying the FM proposed for a four-storey, dual, regularly infilled building resting on type C (Vs=300m/s) soil, for four damage states: Slight Damage (SD), Moderate Damage (MD), Extensive Damage (ED) and Complete Damage (CD).

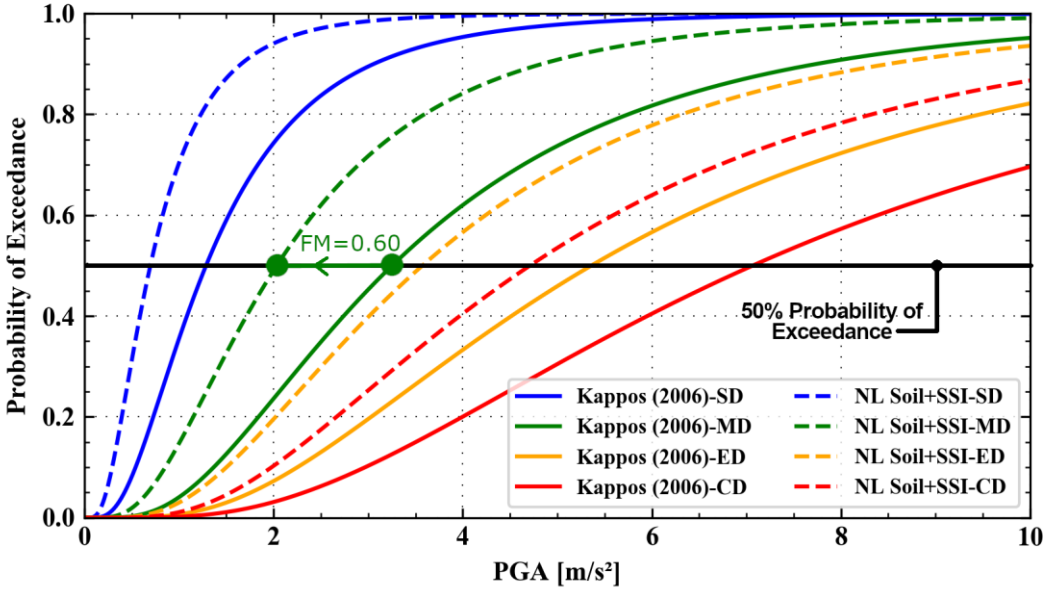

Figure 4. Fragility curves derived by Kappos et al. (2006) and the ones derived applying the FM proposed for a four-storey, dual, regularly infilled building resting on type D (Vs=180m/s) soil, for four damage states: Slight Damage (SD), Moderate Damage (MD), Extensive Damage (ED) and Complete Damage (CD).

Vulnerability curves

To further associate nonlinear soil behavior and SSI with damage and expected losses, we derive the vulnerability product of the presented fragility curves. For this purpose, we select the respective Kappos et al. (2006) damage indices.

Figure 5 shows the loss curve resulting using Kappos et al. (2006) fragility curves and the ones by applying the proposed FM for a four-storey, dual, regularly infilled building resting on type C (V_S=300m/s) soil. Figure 6 shows the loss curve calculated using Kappos et al. (2006) fragility curves and the one by applying the FM proposed for a four-storey, dual, regularly infilled building resting on type D (V_S=180m/s) soil.

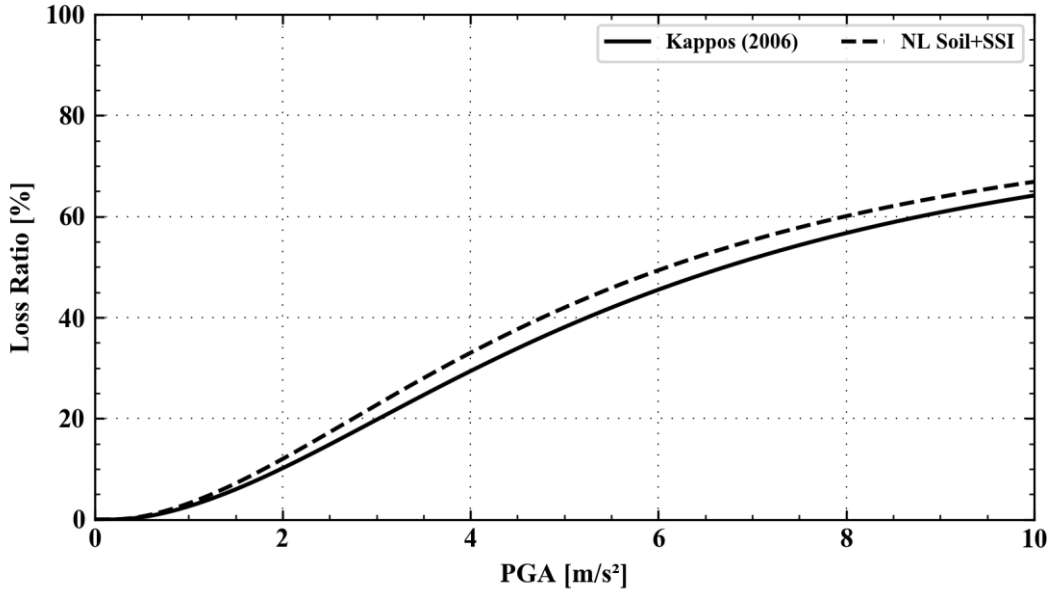

Figure 5. Vulnerability curve derived using Kappos et al. (2006) fragility curves and the one derived applying the FM proposed for a four-storey, dual, regularly infilled building resting on type C (Vs=300m/s) soil.

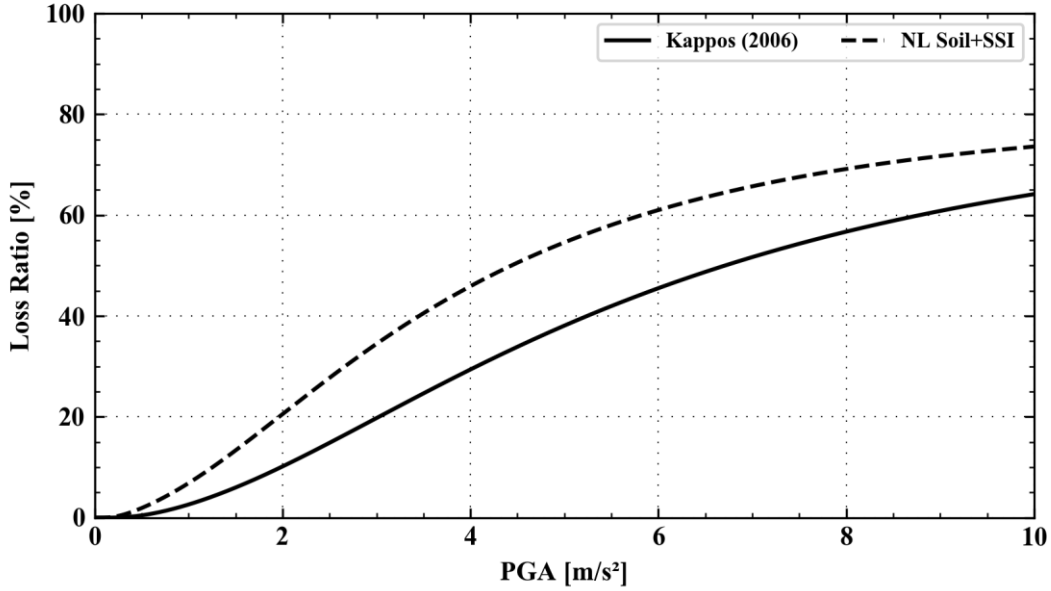

Figure 6. Vulnerability curve derived using Kappos et al. (2006) fragility curves and the one derived applying the FM proposed for a four-storey, dual, regularly infilled building resting on type D (Vs=180m/s) soil.

Discussion

While Figures 3-6 only present some indicative results of the study, the influence of the subsoil conditions is still visible. The FM presented in Figure 2 show that soil nonlinearities and SSI influence fragility, and thus vulnerability, to a larger extent for softer soil profiles. Soil profiles characterized by shear wave velocities >300 m/s usually introduce slight additional losses, from the vulnerability point of view, while softer soil profiles may lead up to 20-30% increase in terms of loss ratio.

According to the FM presented in Figure 2, local site-effects and SSI influence the response of the structures more for the lower damage states (SD, MD), compared to the ED and CD damage states. Moving from lower to higher PGA levels, lower site amplifications are observed, while at the same time, additional SSI-induced interstorey drift influences mainly the SD and MD damage states, defined by low-enough values to be sensitive to slight changes.

Conclusions

An extensive study of earthquake vulnerability of generic RC buildings was performed, focusing on the influence of nonlinear soil behavior and SSI. Results show that subsoil conditions may affect the expected losses to a great extent, highlighting the necessity for a comprehensive modelling procedure that takes into account basic geotechnical parameters. Here we propose fragility modifiers that provide a simplified – yet efficient – scheme of including local site effects and SSI in a large-scale risk assessment procedure.

Acknowledgments

We acknowledge support by the project “HELPOS - Hellenic Plate Observing System” (MIS 5002697) which is implemented under the Action “Reinforcement of the Research and Innovation Infrastructure”, funded by the Operational Programme "Competitiveness, Entrepreneurship and Innovation" (NSRF 2014-2020) and co-financed by Greece and the European Union (European Regional Development Fund).

References

Baker JW (2015), Efficient Analytical Fragility Function Fitting Using Dynamic Structural Analysis, *Earthquake Spectra,* 31: 579–599

D’Ayala D, Meslem A, Vamvatsikos D, Porter K, Rossetto T, Crowley H, and Silva V (2013), *Guidelines for Analytical Vulnerability Assessment - Low/Mid-Rise*, GEM Technical Report, Pavia, Italy

EN 1998-1:2004, *Eurocode 8: Design of structures for earthquake resistance, Part 1: General rules, seismic actions and rules for buildings*, CEN, Brussels, Belgium

GEM (2019). Global Earthquake Model Foundation Official Website. Available at: https://www.globalquakemodel.org (Accessed 16/04/2019)

Kappos A, Panagopoulos G, Panagiotopoulos C and Penelis G (2006), A hybrid method for the vulnerability assessment of R/C and URM buildings, *Bulletin of Earthquake Engineering*, 4(4): 391-413

Karapetrou S, Fotopoulou S and Pitilakis K (2015), Seismic vulnerability assessment of high-rise non-ductile RC buildings considering soil–structure interaction effects, *Soil Dynamics and Earthquake Engineering*, 73: 42 – 57

Mazzoni S, McKenna F, Scott MH and Fenves GL (2009), *Open System for Earthquake Engineering Simulation User Command-Language Manual*, Technical Report, Pacific Earthquake Engineering Research Center, Berkeley, USA

NIBS (2004), *Direct physical damage – General building stock*, HAZUS-MH Technical manual, Chapter 5, Federal Emergency Management Agency, Washington DC, USA

Petridis C and Pitilakis D (2018), Soil-structure interaction effect on earthquake vulnerability assessment of moment resisting frames: the role of the structure. *Proc. 16th European Conference on Earthquake Engineering*, Thessaloniki, Greece

Pitilakis D and Petridis C (2018), Soil-structure interaction effect on earthquake vulnerability assessment of moment resisting frames: the role of the soil. *Proc. 16th European Conference on Earthquake Engineering*, Thessaloniki, Greece

Rajeev P and Tesfamariam S (2012), Seismic fragilities of non-ductile reinforced concrete frames with consideration of soil structure interaction, *Soil Dynamics and Earthquake Engineering*, 40: 78–86

Silva V, Crowley H, Pagani M, Monelli D and Pinho R (2014), Development of the OpenQuake engine, the Global Earthquake Model's open-source software for seismic risk assessment, *Natural Hazards*, 72: 1409–1427

Vamvatsikos D and Cornell CA (2002), Incremental dynamic analysis, *Earthquake Engineering & Structural Dynamics*, 31(3): 491-514

Vamvatsikos D and Cornell CA (2004), Applied incremental dynamic analysis, *Earthquake Spectra*, 20 (2): 523-553

Yepes-Estrada C, Silva V, Rossetto T, D'Ayala D, Ioannou I, Meslem A and Crowley H (2016), The Global Earthquake Model Physical Vulnerability Database, *Earthquake Spectra*, 32: 2567–2585